

1
2 **Continent-Ocean Transition or Boundary? Crowd-sourced seismic interpretations of**
3 **the East-India Passive Margin**

4
5 **Enter authors here: Clare E. Bond¹, Juan Alcalde^{2*}, Robert W. H. Butler¹, Ken**
6 **McDermott³ and Ramon Carbonell²**

7 ¹ School of Geosciences, Aberdeen University, AB24 3UE UK, Aberdeen, United Kingdom.

8 ² Geosciences Barcelona (GEO3BCN), CSIC, 08028, Barcelona, Spain.

9 ³ Shell Global Solutions (UK) Ltd., SE1 7NA, London, United Kingdom.

10
11 *Corresponding author: Juan Alcalde (jalcalde@geo3bcn.csic.es)

12
13 **Key Points:**

- 14 • Passive margin models are conventionally interpreted as abrupt continent-ocean
15 boundaries or diffuse transitions
- 16 • We run a group experiment to explore the range and variability in interpretations of a
17 seismic section from the Eastern India margin
- 18 • Expert elicitation and crowd-sourced experiments are helpful to identify areas of
19 uncertainty within passive margin model building
- 20

21 **Abstract**

22 On the edge of our continents, oceanic crust meets continental crust. At passive margins, those
 23 where there is no active tectonics, subduction or transform faulting, these crustal types are
 24 connected as sharp continent-ocean boundaries (COB) or as diffuse continent-ocean transition
 25 (COT) zones. Passive margins are hard to explore and consequently relatively little is known
 26 about their morphology or the geological processes of their formation. Here we elicit and analyse
 27 seismic image interpretations of the passive margin offshore East India conducted by 17 groups
 28 of geoscientists to better understand the differences, or lack therein, of COB or COT
 29 interpretations of the margin. The group interpretations provide a wide range of margin models,
 30 five of which are abrupt COB based and 11 which are diffuse COT based. However,
 31 interpretations within the COB set vary in the placement of the boundary line between
 32 continental and oceanic crust, the boundary placement lying within the range of interpreted COT
 33 zones, with the average COB location falling in the centre of the interpreted COT zones. These
 34 crowd-sourced results are then compared with ten published interpretations across the margin,
 35 which show COB and COT zones falling in the same area. These findings raise questions as to
 36 the real differences in COB and COT models and the geological processes involved in their
 37 formation. Considering this, we discuss the implications for passive margin models and the use
 38 of Wisdom of Crowds-type approaches in reflecting on both the range of interpretation-based
 39 models and in the value of determining ‘average’ model approaches.

40

41 **1 Introduction**

42 Passive margins are present along the coasts of all continents. Their total length exceeds 105,000
 43 km of the coasts of all continents, constituting the longest tectonic feature and covering circa 7%
 44 of the Earth’s surface (Bradley, 2008; Brune et al., 2016). They also host the thickest
 45 accumulations of offshore sediments (Straume et al., 2019) and contain large amounts of energy
 46 resources (Berndt, 2005; Zhixin et al., 2016), making them important research targets. In spite of
 47 their importance, questions about their constituent form remain.

48 Passive margins are formed by juxtaposed continent and oceanic lithosphere, whether in the form
 49 of sharp or abrupt limits (continent-ocean boundaries, COB) or as more diffuse transition zones
 50 (continent-ocean transitions - COT). These coupling parts of the margins have always attracted
 51 interest; not least because of their implications for rifting and crustal processes (Chian and
 52 Louden, 1994; Blaich et al. 2011; Franke et al. 2011; Peron-Pinvidic et al., 2013), but also
 53 because of how they are used to determine palinspastic reconstructions (Keen and De Voogd,
 54 1988; Seton et al. 2012; Eagles et al. 2015). As Eagles et al. (2015) cover in their comprehensive
 55 review, the definition and demarcation of continent-ocean margins are not well defined, and
 56 scientists frequently propose different margin models for the same area, often even using the
 57 same datasets. It is generally recognised that, in its simplest form, a COB (where continental
 58 crust changes to oceanic crust defined as a linear boundary or line on a map) is a simplification;
 59 whereas as a COT allows for a ‘mix’ of crustal types across a transition zone (an area, or
 60 polygon on a map), and although a range of crustal processes are implied in this transition zone
 61 (e.g. Lavie and Manatschal, 2006; Pindell et al. 2014) they are not necessarily delineated. This
 62 raises issues for palinspastic reconstructions and broader questions on rifting processes that rely

63 on these margin models. Yet these two conceptual models (COB and COT) continue to be used
64 and mapped across a range of continent-ocean margins.

65 To truly confirm abrupt COB or diffuse COT zones and the different process-based
66 interpretations, sampling is required in often very deep, inaccessible or expensive and difficult-
67 to-drill locations (e.g. Sibuet et al., 2007). Therefore, in reality, interpretations and their
68 associated conceptual models are mainly reliant on interpretations of geophysical data: seismic
69 (reflection and refraction), magnetic and gravity data (e.g. Minshull, 2009; Franke, 2013).
70 Interpretations of geophysical data, reflection seismic images in particular, are well documented
71 as being inherently uncertain (e.g. Bond et al., 2007; Alcalde et al. 2017a, 2019; 2022; Pérez-
72 Díaz et al., 2020; Alcalde and Bond, 2022). This uncertainty can create unwanted outcomes, e.g.
73 flawed horizon (Rankey and Mitchell, 2003) and fault (Faleide et al., 2021) interpretations or
74 imprecise interpretation of break-up markers (Causer et al., 2020), that can ultimately lead to
75 inaccurate (COB or COT) margin models.

76 The uncertainty in the interpretation of geophysical data across the continental rift zone of the
77 East-India margin is the focus of this work. This area has been interpreted as both an abrupt COB
78 and diffuse COT margin, which purport, or suggest the possibility of, exhumed mantle at the
79 COB or in the COT zones (Eagles et al., 2015). As well as the difference in the interpretations, it
80 is clear that the mechanisms that underpin the formation of this and other rifted continental
81 margins are still a subject of debate.

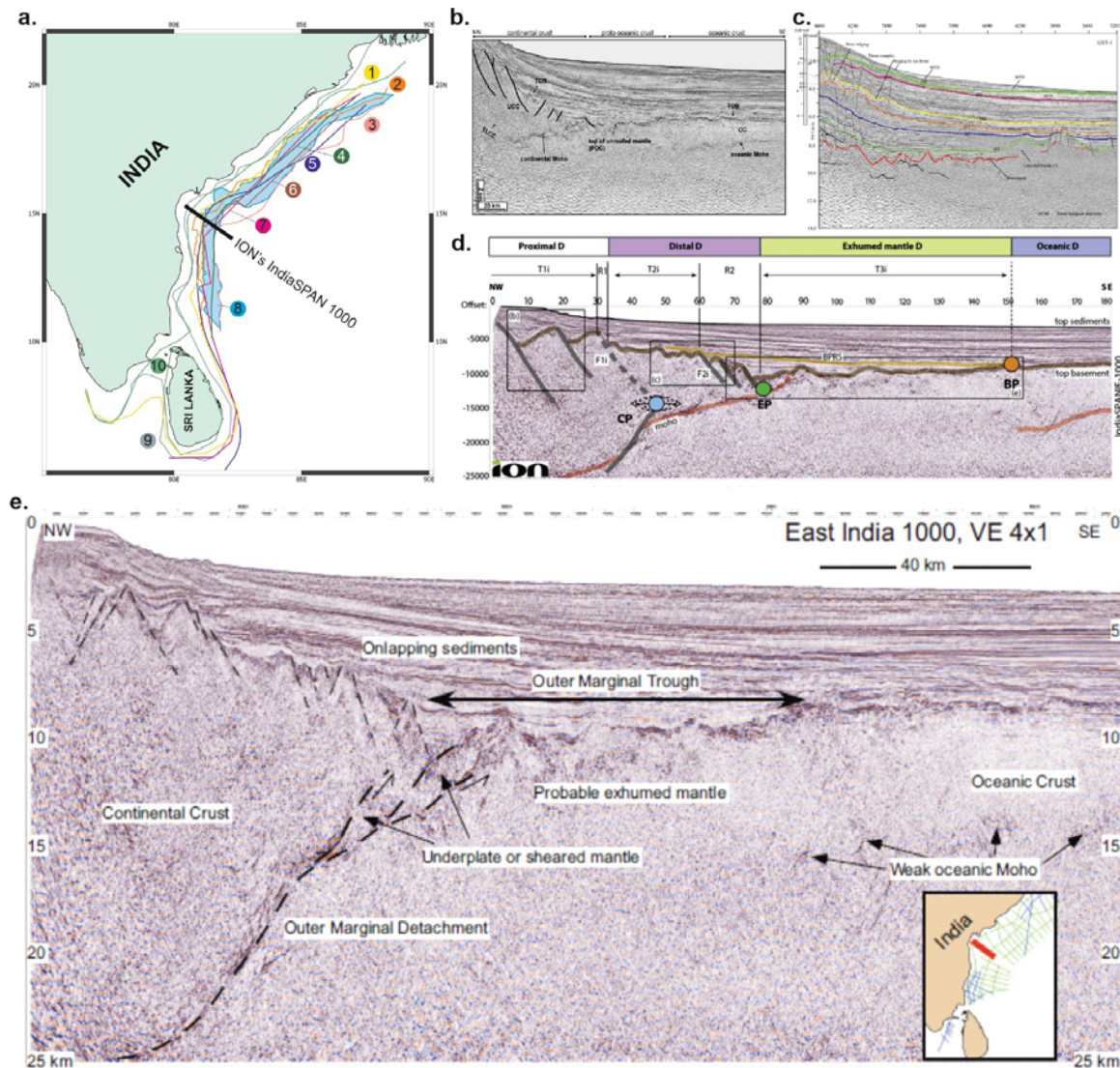
82 Previous interpretation experiments have investigated the value of aggregate individual
83 interpretations to determine an optimal solution(s) (e.g., Bond et al., 2009; 2015; Macrae et al.,
84 2016; Alcalde et al., 2019; Schaaf & Bond, 2019). Instead, here we use a collective of experts'
85 interpretation approach to address this question, a combined "Wisdom of Crowds" and group
86 expert elicitation. The Wisdom of Crowds approach relies on different mechanisms to turn the
87 judgements into a collective outcome or decision (Surowiecki, 2004), i.e., diversity of opinion
88 and experience from the participants involved, independence of ideas, a decentralized approach
89 in which participants draw on their own specialist knowledge, and make an effective aggregation
90 of the results. We draw on these aspects, but our crowd are experts (geoscientists) and perform
91 the interpretation in small groups.

92 In this work, we explore the range in interpretations of a single 2D regional seismic dataset from
93 the East-India margin by several groups of geoscientists. The experiment presented in this work
94 originated from multiple interpretations of this seismic dataset, providing an excellent example
95 through which to test the variety in interpretations and the competing hypotheses on which they
96 are based. It also allows the question to be posed of if the different interpretations can, or cannot,
97 be used collectively to determine broad model suites. The aim of the experiment was to explore
98 the range in interpretations to a single dataset, to understand which parts of the data yield similar
99 interpretations and which are more contested. The use of a single 2D seismic image allows us to
100 better constrain the range in interpretations, without the additional uncertainty associated with
101 different input datasets that Eagles et al. (2015) recognise as a likely factor in their review of
102 interpretations across the East Indian margin. We observe a range in interpretations across our
103 participant groups, to quantify the difference in abrupt COB and diffuse COT interpretations and
104 to see if the average COB and COT interpretations (i.e. the Wisdom of the Crowd) could be
105 thought of as representative of the interpretation set(s) and if they are geologically reasonable.

106 2 The East-India margin

107 The East-India passive margin formed as a result of the breakup between Antarctica and the
 108 Indian subcontinent during Early Cretaceous time (Powell et al., 1988; Haupert et al., 2016). The
 109 subsurface of the East-India margin is well imaged by seismic data, and has been the focus of
 110 numerous interpretations. Several of these interpretations (Powell et al. 1988; Rao et al. 1997;
 111 Bouysse et al, 2009; Krishna et al., 2009; Veevers, 2009; Bastia et al. 2010; Sinha et al. 2010;
 112 Seton et al. 2012; Gibbons et al. 2013; Nemčok et al. 2013) are included in the overview of
 113 Eagles et al. (2015; their figure 10); redrawn here (Figure 1a) to show the range of
 114 interpretations for the margin. Note that papers published in 2014 and onwards are not included
 115 in the overview of Eagles et al. (2015). Eagles et al. (2015) calculate a mean width of the COB of
 116 184 km, standard deviation of 79 km, measured along 16 equally spaced transects.

117



118

119 **Figure 1.** Location map and seismic section used in this experiment. a) The East Indian margin
 120 with the location of the ION's IndiaSPAN 1000 marked, and data showing the location of COB
 121 and COT interpretations redrawn from Eagles et al. (2015). The numbers indicate the
 122 interpretation sources as follow: 1 – Bouysse et al., (2009); 2 – Bastia et al. (2010); 3 - Sinha
 123 (2010); 4 - Rao et al. (1997); 5 - Krishna et al. (2009); 6 – Veevers (2009); 7 – Powell et al.
 124 (1988); 8 - Nemčok et al. (2013); 9 – Gibbons et al. (2013); 10 – Seton et al. (2012). b), c), d)
 125 and e) The Ion East India 1-1000 seismic section interpreted by Nemčok et al., (2013), Haupert
 126 et al. 2016, Mangipudi et al., (2014) and Pindell et al. (2014), respectively. Note that the
 127 numbers in a) do not correspond to the number codes in Eagles et al (2015).

128
 129 This study focuses on the interpretation of the ION's IndiaSPAN-1000 2D regional seismic line.
 130 This seismic dataset comes from the offshore Andhra Pradesh part of the margin and extends
 131 over 200 kms (Figure 1a). This line has been interpreted in five recent papers (Sinha et al., 2010;
 132 Nemčok et al., 2013; Pindell et al. 2014, Mangipudi et al. 2014, Haupert et al. 2016) (Figure 1b-
 133 e). Sinha et al. (2010) and Nemčok et al., (2013) define a COT zone as a “proto-oceanic crust”,
 134 featuring c. 50 km of “exhumed” and “unroofed” mantle, respectively. Mangipudi et al. (2014)
 135 also describe an area akin to unroofed mantle, reported in similar areas with interpreted proto-
 136 oceanic crust. For Haupert et al. (2016) the exhumed mantle is extensive and indicative of
 137 hyperextension processes (Lavier and Manatschal, 2006). For Pindell et al. (2014) exhumed
 138 mantle is “possible” and they suggest an additional primary stage in passive margin formation,
 139 ‘outer marginal collapse’ occurring after the traditional rift stage and before the thermal
 140 subsidence stage that they describe as encompassing the collective processes that form COT
 141 zones. Nemcok et al. (2013) provide the only COT interpretation of this dataset, with a 20-100
 142 km transition zone interpreted along the margin.

143 **3 Group interpretation experiment**

144 Interpretation of the ION's IndiaSPAN-1000 2D regional seismic line (like that shown in Figures
 145 1c and 1e but uninterpreted and unannotated) was conducted during the 17th International
 146 SEISMIX Conference, held in May 2016 in Aviemore, Scotland. The participants were
 147 geoscientists (chiefly geophysicists and geologists with expertise in seismology) attending the
 148 conference. Interpretation of the seismic line was conducted through a facilitated workshop.
 149 Participants self-assigned themselves into groups of three to five people, with 17 groups
 150 completing the interpretation in total. Each group was given a deep seismic profile provided by
 151 Ion, that had been migrated and depth converted. The seismic profile was presented as a hard
 152 copy print in colour with vertical and horizontal scales equal, shown in km at a scale of 1:1. The
 153 only annotation on the image were the scale. The participants were not told where the seismic
 154 profile was from, nor were there presentations (oral or poster) before the experiment that
 155 discussed the image or the tectonics of continental rifting. The India-SPAN-1000 2D seismic line
 156 has a high quality and therefore provides the best opportunity to minimise interpretational
 157 uncertainty associated with image quality (Alcalde et al. 2017b; Alcalde et al., 2017c).
 158 Confidentiality reasons mean we cannot share this image with readers, but images of the line
 159 (with different display characteristics) have been published (Figure 1). A printed instruction

sheet that explained the exercise and asked the participants as a group to interpret the image. The instructions included a preamble to explain the scope of the experiment, general information about the seismic line and about the author's commitment to keep the results anonymised.

To ease comparison between the different interpretations, the groups were asked to identify the following four features: (i) different crust (basement) types – i.e., continent vs oceanic crust; (ii) different sedimentary units – e.g. pre-, syn- and post-tectonic units; (iii) the Moho – under the continent, the ocean and whether/how these connect; and (iv) the presence of faults. The full set of instructions are available in the supplementary material.

Each group were also asked in the instructions to complete a questionnaire. The questionnaire was designed to elicit the groups' knowledge of the specific seismic image they were being asked to interpret, as well as of rifted margins more generally and the groups experience in seismic interpretation. The collated information is summarised in **Annex 1**. The groups consisted of individuals with a range of seismic interpretation expertise and backgrounds in rifted margins. Importantly, none of the groups had worked on, or recalled having seen the seismic image previously. This means that comparison between the different groups' interpretations is more robust, with no individual or group carrying a specific bias or expectation from having seen or worked on the data previously. The participants were encouraged to be proactive and cooperative within the interpretation exercise.

178

179 **4 The Wisdom of Crowds approach**

180 The Wisdom of Crowds (Surowiecki, 2004) builds on the hypothesis that the combination of
181 multiple judgements outperforms individual assessments (Budescu & Chen, 2015). A highly
182 successful example of Wisdom of Crowds is Wikipedia, which has substituted traditional
183 encyclopaedias thanks to its open access, collaborative approach (Kittur and Kraut, 2008).
184 Surowiecki (2004) outlined four key criteria for a successful Wisdom of Crowds approach,
185 namely diversity, independence, decentralization and aggregation approach. Below is a
186 description of these four elements and their fit in our interpretation experiment.

187 i) **Diversity** in opinion and expertise. Each participant should add their own point of view to the
188 interpretation, as it is well accepted that diversity in expertise and viewpoints enhances creativity
189 and problem solving (e.g. Kelley and Tibaut, 1954; Hoffman and Maier, 1961; Larson Jr, 2007).
190 By running our seismic interpretation experiment at the international SEISMIX conference, we
191 aimed to ensure a diverse mix of individuals with different backgrounds and experience. Across
192 the groups there were some “super experts” (i.e., had completed research in these settings),
193 whilst others had less experience. Collectively, the experts in this experiment could be described
194 as seismologists with a range of expertise in application, from signal and data processing relating
195 to various seismic techniques through to geological interpretation of seismic (chiefly reflection)
196 imagery. Each participant could contribute to the interpretation based on their different expertise.

197

198 ii) **Independence**, so that individuals' opinions are formed independently. Participants should be
199 able to provide their opinions without being conditioned by the opinions of the rest of the
200 members of the group. In other words, care must be taken so that the Wisdom of the Crowd
201 prevails over herding bias (Larrick et al., 2012). For this element, we did not follow a Wisdom of
202 Crowds approach and the experiment was undertaken as a group exercise, and we acknowledge
203 that within any individual group, the opinions of individuals will have been tempered by others
204 and the group view. However, we ensured that the 17 groups operated independently with
205 interpretation sharing and discussion only after completion of the interpretation. We used the
206 collective interpretation of each group as a data point or set (e.g. as though created by an
207 individual); although we recognise that dominance of specific individuals, and personality traits
208 within the groups will likely affect the collective outcome (see Polson and Curtis, (2010), for a
209 geoscience example of group decision making dynamics). The collective experience of each
210 group can be seen in Annex 1.

211 iii) **Decentralization**, where people draw on their own specialist knowledge. By running the
212 experiment at SEISMIX individuals were free from the normal constraints of their working
213 practices and colleagues. This decentralized approach would likely result in greater diversity
214 than for example running the exercise with a group of geoscientists from the same company in
215 their usual working environment. Although groupings were self-assigned the experiment
216 coordinators encouraged participants to form groups with people they did not know or with
217 which they did not commonly collaborate, to enhance diversity, independence and
218 decentralization within the groups.

219 iv) **Aggregation**, an effective mechanism to turn the judgements into a collective decision. As
220 the majority of the information, we collected is geo-spatial we used a simple image stacking
221 approach in order to determine the range in interpretations, and the mean response. This process
222 is outlined further in the results section.

223 Our experiment differs from that of a classic Wisdom of Crowds approaches is that in the
224 traditional examples (e.g. estimating the weight of a Bull at an agricultural fair) there is a single
225 unequivocal answer to the question posed. In our interpretation example there is not a single
226 deterministic solution and indeed two independent conceptual models dominate known thoughts.
227 So here we use the wisdom of the collective-experts slightly differently, not to determine the
228 solution to a simple question with a singular answer, but to address three important questions: (i)
229 to see if the experts wisdom represents the two known dominating models; (ii) to investigate how
230 independent these two models actually are in practice; and (iii) to assess the use the collective
231 wisdom of the experts to determine an optimal interpretation solution or solutions for the
232 interpretation of this seismic dataset. In summary, we are using a Wisdom of Collective Experts
233 approach to explore the diversity in interpretation and what that means for the conceptual models
234 of an abrupt COB or a diffuse COT zone.

235

236 **5 Interpretation results**

237 The collated interpretations were initially assessed for the four different features that the groups
 238 had been asked to identify in the interpretation instructions (i.e. the Moho, the basement, the
 239 faults and the different types of crust) (Table 1). All groups identified the Moho, all but one
 240 group had interpreted faults in the sedimentary cover sequence and similarly crustal types. Two
 241 groups chose not to identify pre-, syn-, and post-rift mega sequences, see summary of identified
 242 features in Table 1. Using the key features identified in the interpretation instructions, and other
 243 commonly identified elements (e.g. exhumed mantle, thinned or hyper extended continental
 244 crust, continent-ocean transition zones, see Table 1 for the full list) the interpretations were
 245 divided into the binary ‘model types’ an abrupt relationship – COB or a diffuse one (COT).
 246 Figure 2 shows examples of the group interpretations. Of the 17 group interpretations, 11 groups
 247 (65%) explicitly defined a continent ocean transition (COT) zone. For the five groups that made
 248 a COB interpretation (29%), two of the groups marked a boundary, whilst in the other three cases
 249 continental crust was identified distinctly from oceanic crust, so the COB categorisation and
 250 boundary is implicit from the joining point rather than explicitly identified. Only one group did
 251 not provide enough evidence for categorisation into either of the binary model types.

252

253

Group	Specifically requested in the instructions							Other features interpreted								Data Artefact	
	C-O margin		Moho	Number of faults	Faults	Crust types			Sedimentary units			Thinned or hyperextended Continental Crust	Exhumed mantle	Serpentinised Mantle	Underplating Intrusions	Salt	Subduction
	Pre-rift	Syn-rift	Post-rift														
JJ	COT	Y	10	Y	Y	Y	Y	Y		N	N	N	N	N	N	N	N
JK	COT	Y	14	Y	Y	Y	Y	Y		Y	N	N	N	N	N	N	N
JL	?	Y	6	Y	N	N	N	N		N	N	N	N	N	N	N	N
JM	COB	Y	10	Y	Y	N	Y	Y		N	N	N	N	N	N	N	Y
JN	COT	Y	11	Y	Y	Y	Y	Y		N	Y	Y	N	N	N	N	Y
JP	COT	Y	6	Y	Y	N	N	N		N	N	N	N	N	Y	Y	N
JQ	COT	Y	33	Y	Y	N	Y	Y		Y	N	N	N	N	N	N	Y
JR	COB	Y	12	Y	Y	Y	Y	Y		Y	Y	Y	N	Y	N	N	Y
JS	COT	Y	1	Y	Y	N	N	Y		Y	Y	Y	N	N	N	N	N
JT	COT	Y	12	Y	Y	N	Y	Y		Y	N	N	N	N	N	N	Y
KJ	COT	Y	-	N	Y	Y	Y	N		Y	N	N	N	N	N	Y	N
KK	COB	Y	10	Y	Y	N	Y	Y		N	N	N	N	N	N	N	N
KL	COT	Y	8	Y	Y	N	Y	N		N	N	N	N	N	N	N	N
KM	COT	Y	10	Y	Y	N	Y	Y		N	Y	Y	N	N	N	N	N
KN	COB	Y	14	Y	Y	N	N	N		N	N	N	Y	N	N	N	N
KQ	COB	Y	6	Y	Y	Y	Y	Y		Y	Y	N	N	N	N	N	N
KR	COB	Y	20	Y	Y	N	Y	Y		N	N	N	Y	N	N	N	N
Percentage of Y		100%	-	94%	94%	35%	76%	65%		41%	29%	24%	18%	12%	6%	12%	29%

254

255 **Table 1.** A summary of the features interpreted by the 17 different groups. The table is divided
 256 into those features specifically requested in the interpretation instructions and other features
 257 interpreted by the groups (column 1) that have been used to define the ‘binary’ model type (COB
 258 or COT) interpreted (column 2); Y=yes interpreted, N=Not interpreted.

259

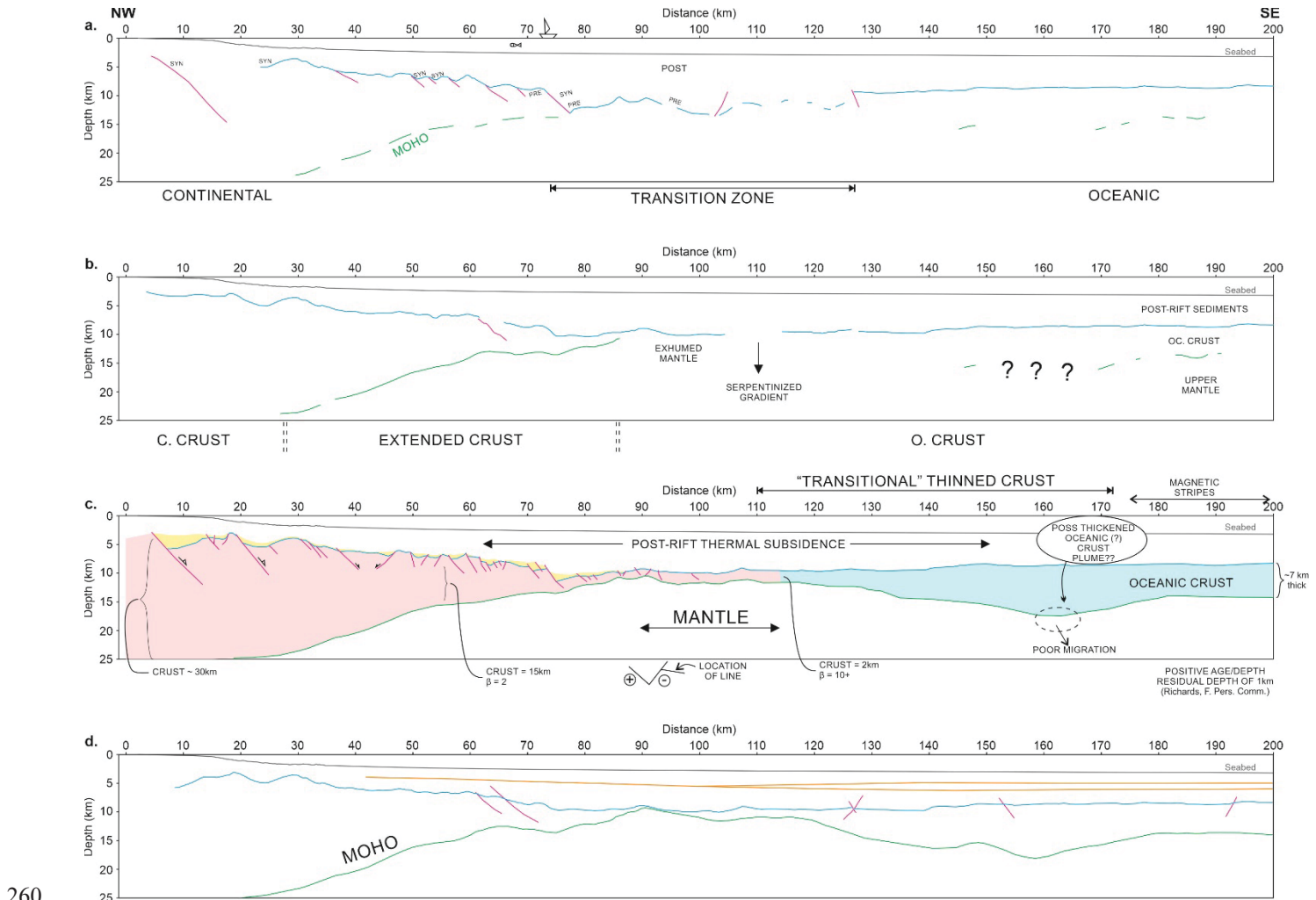


Figure 2. Digitised examples of the different group interpretations. a) COT interpretation (group - JJ), with the extent of the transition zone marked by an arrowed section. The Moho is partially interpreted, as is the top of the Basement. b) COB interpretation (group - JS). This interpretation has the extended crust annotated, as well as exhumed mantle. The Moho is partially interpreted and uncertainty in its position is marked by question marks. c) COT interpretation (group - JQ). The interpretation uses annotation to show the extent of 'transitional' thinned crust; the thickness of the continental crust and the oceanic crust and associated β - stretching factors, as well as other features. d) The one interpretation (group - JL) that could not be categorised. The interpretation shows the Moho, Top Basement, Faults and sediment fill; but with no identification of oceanic or continental crust, a boundary or a transition zone.

After categorisation into abrupt COB interpretations or diffuse COT, we measured the distance of the boundary or transition from the beginning of the seismic section. Note that all distances are measured left-right (i.e. NW-SE) from the continental crust end of the section. For the group interpretations categorised as COB, the interpreted end of the continental crust and the start of

277 the oceanic crust ranged in location from 75 km-142 km along the section, with a mean value of
 278 101 km and a median of 93 km (Table 2a). For the group interpretations categorised as having
 279 COT zones, calculations were made of the extent of the transition zone that had either been
 280 indicated directly, or that could be inferred from the marked extents of the continental and
 281 oceanic crust in each interpretation (Table 2b). For the COT interpretations, the length of the
 282 transition zone ranged from 24 km-84 km, with a mean value of 44 km and a median of 38 km.
 283 The interpreted position of the start of the transition or end of the continental crust along the 200
 284 km long seismic section ranged from 43 km-110 km with the oceanic crust or end of the
 285 transition zone starting between 67 km-172 km.

286

a.	Group/reference	COB (distance in km)	Method	b.	Group/reference	length	COT (distance in km) start	end	Method
Group COB Interpretations	JM	75	Re	Group COT Interpretations	KL	24	43	67	Re
	JS	86	Re		KJ	84	51	135	Re
	KQ	86	Re		JJ	53	74	127	Re
	KR	127	Re		JP	65	76	141	Re
	KN	142	Re		JT	38	76	114	Re
	9	11	G		JN	47	80	127	Re
	10	28	G		JK	58	83	141	Re
	2	59	G		KM	38	85	123	Re
	1	70	U		KK	30	87	117	Re
	5	82	G		JR	14	109	123	Re
Literature COB Interpretations	6	103	Ra		JQ	62	110	172	Re
	7	123	Ra		8	76	62	138	G,Re
	4	127	G,M,Re						
	3	135	U						

287

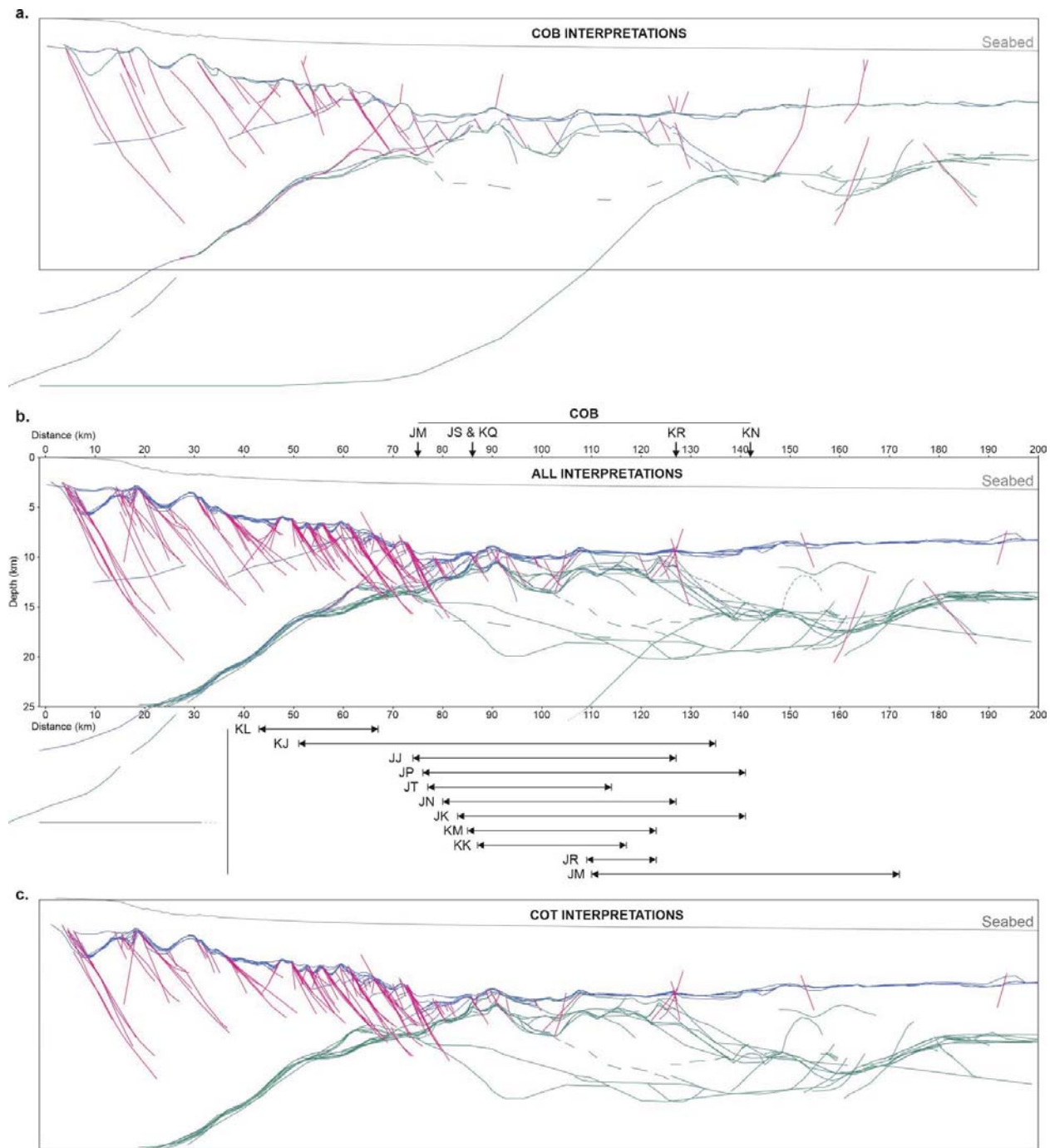
288 **Table 2.** The interpreted positions of the COB and COT zone along the seismic section. a) Interpreted positions of the COB from groups in this study and from the literature measured
 289 along the seismic section. b) The interpreted length and start and end points of the COT zone
 290 from groups in this study and the literature, along the seismic section. The distances refer to the
 291 position with respect to the beginning (i.e. NW, left handside of the seismic image) of the Ion
 292 IndiaSPAN 1000 seismic line. See Figure 1 for literature reference numbers. The “Method”
 293 column indicates the method used to estimate the COB or COT in the literature interpretations,
 294 as reported in Eagles et al (2015): G – gravity data; M – magnetic data; Ra – refraction seismic
 295 data; Re – reflection seismic data; U – unknown source.

297

298 For each groups’ interpretation three elements were manually digitised: the Moho, Top
 299 Basement and any interpreted Faults. The digitisation provided a suite of interpretations that are
 300 easily compared in standard software graphics packages. We used the software Corel Draw
 301 (www.coreldraw.com) to stack the interpretations (Figure 3b) for comparison. This initial
 302 stacking allowed a precis of the range in the 17 different group interpretations, including
 303 assessment of evidence for differences in interpretation of these three specific elements. We were
 304 particularly interested in differences in interpretations between the two categorisations (COB and
 305 COT) of interpretations (Figure 3a and c); and how interpretation inference, and annotations, of
 306 the crustal processes are reflected in the interpretation of these elements. We also generated heat

maps of interpretation intensity (Figure 4), using the software Image J (Schneider et al. 2012). In these maps, areas with great number of overlapping interpretations (or greater interpretation intensity) are highlighted over a white background of no interpretations. This way we can use these heat maps to identify areas where participants interpreted the same (i.e. high intensity) or different (low intensity) features. Using these two methods, we consider each of the interpreted elements in turn.

313



314

315

316 **Figure 3.** Digitised and stacked group interpretations. a) The five COB interpretations stacked.
 317 b) All 17 group interpretations stacked. The position of the COB as identified by the five groups
 318 is annotated above the stacked interpretations, and the extent of the COT zone for the 11 COT
 319 group interpretations is shown below the stacked interpretations. c) The 11 COT interpretations
 320 stacked. In each subfigure the Moho is green, Top Basement is blue and Faults are magenta.

321 *The Moho*

322 Interpretation of the Moho (green lines in Figure 3, and as a heat map Figure 4a and 4b), shows
 323 consistency in interpretation in all groups, bar two, under the continental crust at the start of the
 324 section. The two groups with differing interpretations are both abrupt COB interpretations, one
 325 shows the Moho starting to deepen from c.140 km toward the continental crust end of the
 326 section, the other shows the Moho deeper than other interpretations at the continental end of the
 327 section (0 km). There is also relatively good correlation of Moho interpretations under the
 328 oceanic crust at the far end of the section. These areas are less equivocal than the central part of
 329 the section where the continental crust ‘joins’ the oceanic crust. None of the COB interpretations
 330 show the Moho reaching the Top Basement, indicating that mantle has not been fully exhumed
 331 and therefore do not support a fully hyper-extended rifting model that brings mantle to the
 332 surface. In contrast, several of the diffuse COT interpretations show this to be the case with
 333 mantle being exhumed to the surface covered only by syn- and post-rift basin fill. In all the
 334 interpretations the Moho is relatively shallow, resulting in a significantly thinned crust even
 335 where mantle is not exhumed.

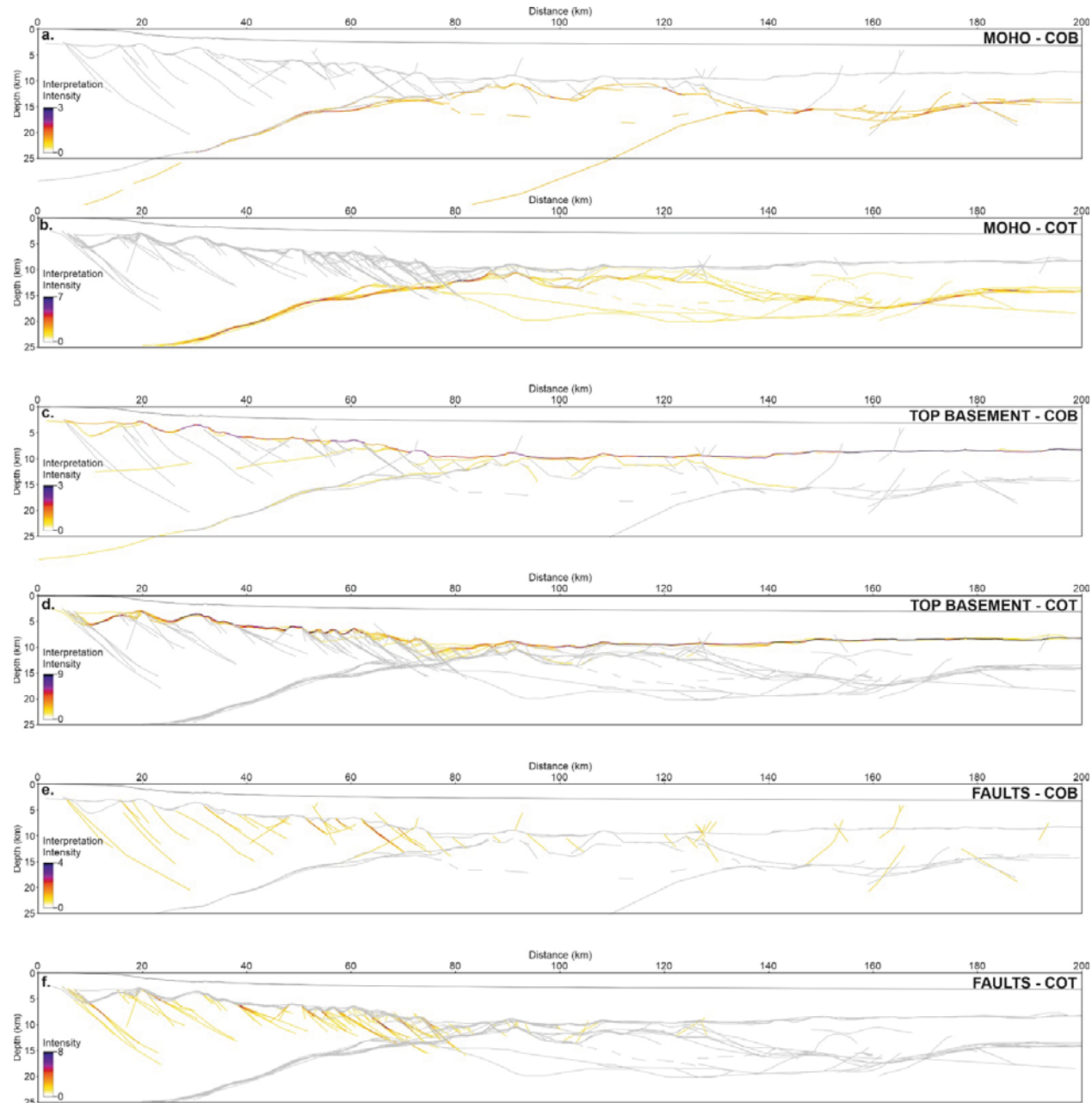
336 *Top Basement*

337 Variation in the interpretation of Top Basement is limited (Figure 4c and 4d), although two
 338 interpretations have a much deeper Top Basement than the others. These two groups (JM and
 339 KN) are both abrupt COB interpretations (Figure 4c) and also interpreted a deeper Moho than
 340 other groups (Figure 4a). Bar these two groups, most of the group interpretations conform with
 341 minor discrepancies in areas where basement faulting has or has not been interpreted. This is
 342 particularly evident between 60 and 90 km on the seismic line. This is around the point where
 343 interpretations mark the start of a transition zone or the edge of continental crust (Figure 3b).

344 *Faults*

345 Fault interpretations were mainly concentrated in the continental crust (Figure 3). The majority
 346 of the interpreted faults dip basin-wards accommodating extension during rifting. Fault
 347 interpretation in the central and farthest (i.e. ocean-ward) part of the section is varied, with
 348 examples of faults dipping both towards and away from the continental margin. Where the crust
 349 is interpreted by all group to be its thinnest faulting is not ubiquitous or dominant and the
 350 mechanism for crustal thinning in this zone is therefore unclear. The lack of fault interpretations
 351 in this zone maybe because the resolution and clarity of imaging in this part of the seismic is not
 352 as clear as elsewhere (see Figure 1e), and/or due to the short extent of any possible faults so that
 353 the groups did not bother to interpret them. Fault dip measurements of 143 interpreted faults

354 (including antithetic faults) in the continental crust ranged from 15-90° with a mean fault dip of
 355 38°, lying within the expected value range for normal fault dips accommodating rifting. There is
 356 no change in the fault dip of those faults that were interpreted where the crust is at its thinnest
 357 and where the abrupt COB and diffuse COT zone interpretations fall.



358
 359 **Figure 4.** Heat maps of the three elements (Moho, Top Basement and Faults) that the groups
 360 were requested to interpret, split by abrupt COB and diffuse COT model types. Moho heat maps
 361 of the COB (a) and COT (b) interpretations. Top Basement heat maps of the COB (c) and COT
 362 (d) interpretations. Fault heat maps of the COB (e) and COT (f) interpretations. In all images, the
 363 heat map intensity colour bar is scaled to the maximum number of overlapping interpretations in

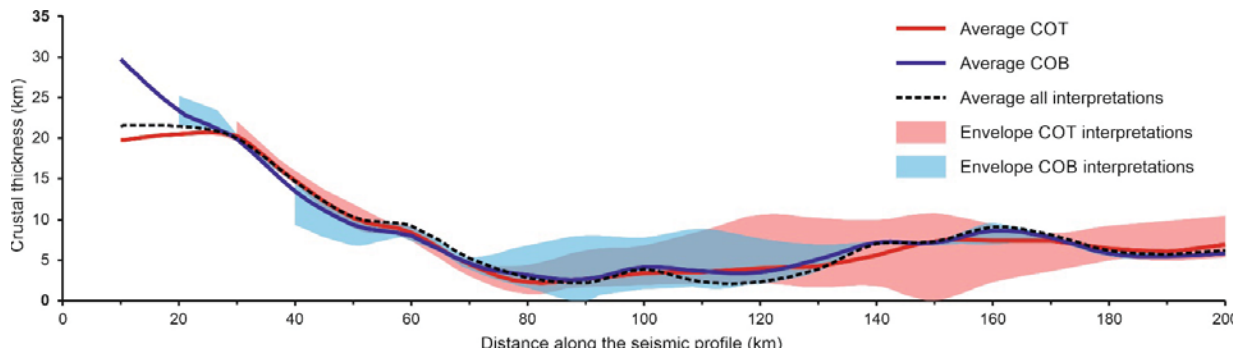
364 the set for the element of interest. In each instance the other elements interpreted as well as the
 365 seabed are shown in pale grey.

366 **6 Crustal thinning calculations**

367 For all fourteen interpretations with Top Basement and Moho interpreted, a crustal thickness
 368 value was calculated. This calculation was completed in Move software by unfolding the Moho
 369 to a horizontal template line using a vertical simple shear algorithm and passively unfolding Top
 370 Basement to create a thickness profile. The combined thickness profiles for the 14 interpretations
 371 are shown in Figure 5, split by COB and COT margin types. The interpreted crustal thickness
 372 ranges from 30 km at the continental end of the section to zero in the COB/COT zone, with a
 373 range of oceanic crust thickness of 5.5–10.5 km, and an average of 6 km. The five COB
 374 interpretations range from 30 km (continental crust) through a minimum crustal thickness of 0
 375 km and have an average oceanic crustal thickness of 5.7 km; whilst the nine COT interpretations
 376 range from a maximum 22 km thickness for the continental crust (note that there are few full
 377 interpretations at the left hand-end, continental crust, of the section) through a minimum
 378 continental crustal thickness of 16.3 km and an average oceanic crustal thickness of 6.9 km.

379 Apart from at the left-hand end of the section, where only one interpretation of each margin type
 380 are available, the abrupt COB and diffuse COT interpretations give very similar average crustal
 381 thickness. These averages always lie within the range of both the COB and the COT based
 382 interpretations (blue and red envelopes, respectively, Figure 5). The interpreted continental
 383 crustal thickness decreases rapidly, from an interpreted maximum of c. 30 km to less than 5 km
 384 over 70 kms, through a combination of fault-based rifting and crustal thinning. The range in the
 385 crustal thicknesses calculated from the interpretations gives an indication of the uncertainty in
 386 the groups' interpretations for the Top Basement and Moho. Diffuse COT interpretations show a
 387 greater range in interpretations of thickness for the oceanic crust than the abrupt COB
 388 interpretations, presumably resulting from differences in interpretations of the extent of the
 389 transition zone and the associated underpinning processes. In the area defined by the range in
 390 COB interpretation points (c.75–140 km) and the average COT transition (c.80–130 km) (Figure
 391 6), the envelopes of both the abrupt COB and diffuse COT crustal thickness interpretations show
 392 a spread indicative of uncertainty in crustal thickness of up to 10 km.

393
 394



395

396 **Figure 5.** Average crustal thickness interpreted across the section showing the average for all
397 interpretations (dashed line), the average for the diffuse COT (red line) and abrupt COB
398 interpretations (blue line) separately, and the envelopes of the range in thickness interpreted.
399 Crustal thicknesses were calculated every 10 km along the seismic section for each
400 interpretation.

401 **7 The crowd-sourced interpretations**

402 An overall '*average*' interpretation was created from all 17 interpretations, as well as *averages*
403 for the abrupt COB and diffuse COT interpretations separately (Figure 6). These averaged
404 interpretations were created by picking the highest intensity trace of each of the three elements
405 (Moho, Top Basement and faults) from the heat maps (Figure 5). Thus, they are not averages in
406 the true sense of the word, but frequency derived, and hence modes or modal interpretations.
407 Modal interpretations can only be created if two or more interpretations overlap. Modal
408 interpretations of the Moho and Top Basement across the seismic image were created without
409 issue, but the number of faults and their placement on the section line by each group varied. In
410 total, 143 faults were interpreted across the seismic section by all groups, many of which were
411 only interpreted by one group; the resulting fault modal model only contains those interpreted by
412 two or more groups.

413 The modal interpretations result in a model where the crust in the central section of the
414 interpretation is significantly thinned. This corresponds with the average extent of the transition
415 zone across all of the COT interpretations, extending from 80–125 km along the section (Figure
416 6b). In this zone, the average crustal thickness is fairly constant, with a range of 2.2 – 3.8 km and
417 an average of 2.7 km. The middle point of this transition zone falls approximately at the point of
418 the average placement of the continent ocean boundary in the abrupt COB models (Figure 6a),
419 the middle of the seismic profile. The geometries of the Moho and Top Basement are generally
420 similar, including the broadly stepped profile observed in the Moho. The major difference is
421 observed at the start of the thickening of the oceanic crust, which is gentler in the modal COB
422 model and steeper in the modal COT model and coincident with the end of the transition zone.
423 The modal COT interpretation has a greater number of faults interpreted than the modal COB
424 interpretation. This is probably partly due to the greater number of diffuse COT than abrupt COB
425 interpretations in the dataset.

426

427

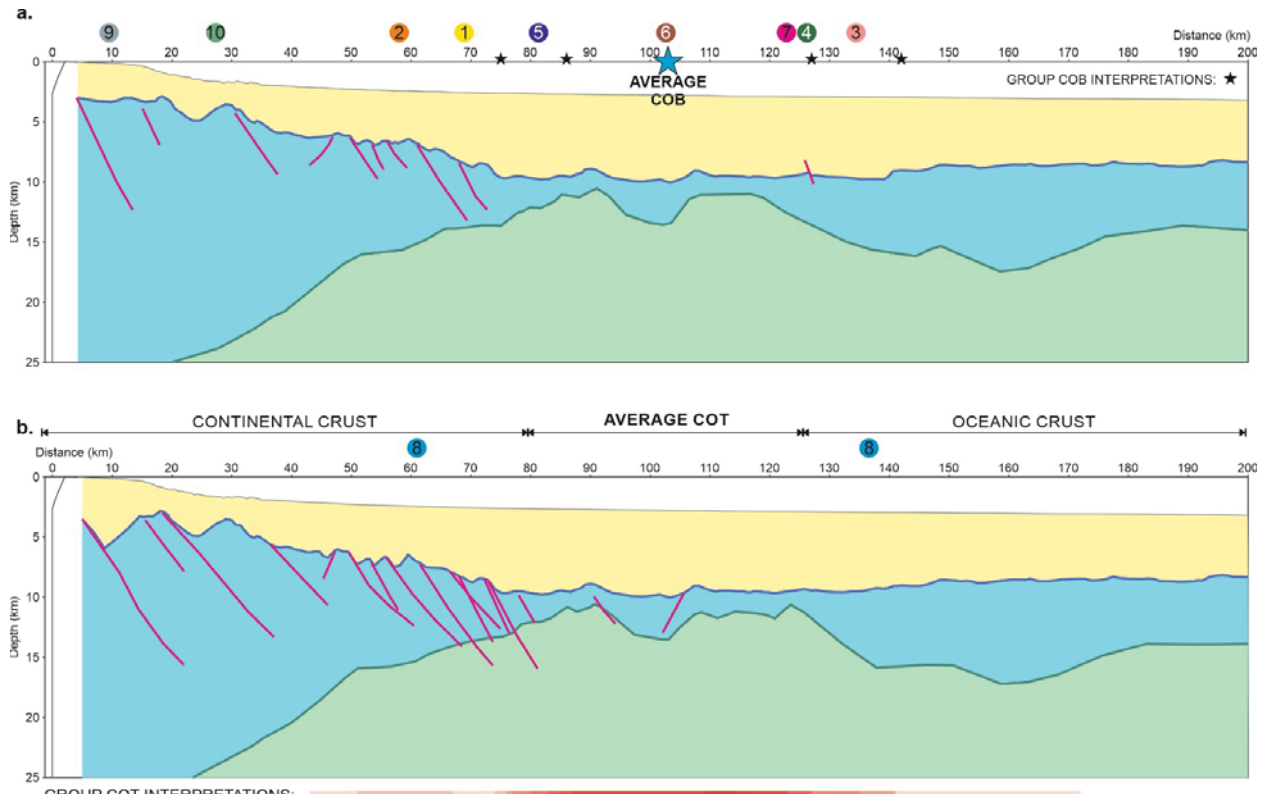
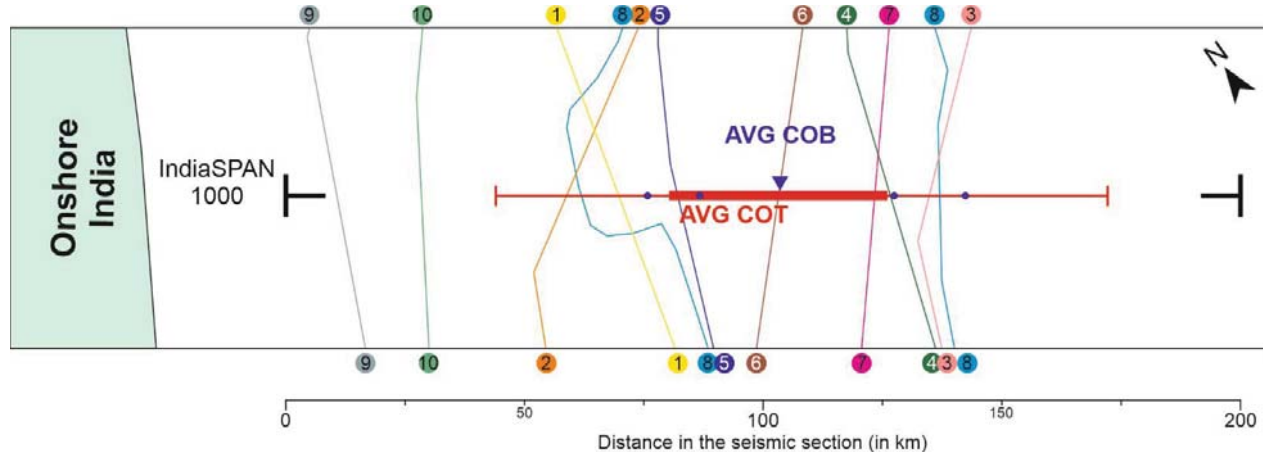


Figure 6. Modal interpretations calculated from all groups for abrupt COB and diffuse COT models, including the sedimentary units (yellow), the basement (blue) and the upper mantle (green). a) Modal interpretation calculated from the five COB model interpretations. The position of the average COB is shown with a blue star, individual COB position interpretations are marked with smaller black stars (see also Figure 3b). b) Modal interpretation calculated from the eleven COT model interpretations (calculated as the average start and average end of the COT interpretations). The extent and position of group interpretations of the COT zone are represented below the section as an intensity colour bar, the higher the colour intensity (red) the more groups interpreted a transition zone in that portion of the seismic section (see Figure 3b for individual group transition zone extents). Interpretation colours follow previous figures: Moho – green, Top Basement – blue, Faults - magenta. The coloured numbers represent the placement of COB and COT interpretations across the East Indian Margin from the published studies outlined in Eagles et al. (2015) and summarised in Figure 1.

We also compare the group interpretations elicited in this study with those previously published for the margin, as summarised in Figure 1. Figure 7 shows this comparison in a schematic map view. Eight of the published interpretations lie within the range of the 17 group interpretations elicited for this study. They also span (symmetrically) the average COB and COT range (calculated as the average start and average end of the COT interpretations) and, if included in our analysis, they would not significantly modify these averages. Two of the published interpretations, those reported in Gibbons et al. (2013) and Seton et al. (2012), are located closer

450 to the coast of India, outside the range of COT interpretations (interpretations 9 and 10 in Figure
 451 7).

452



453
 454 **Figure 7.** Schematic map view of the placement of abrupt COB and diffuse COT interpretations
 455 across the East Indian Margin from the published studies outlined in Eagles et al. (2015) and
 456 summarised in Figure 1. Numbers refer to the different publications (see Figure 1 caption).
 457 Analysis of the 17 group interpretations elicited in this study are represented by an average COB
 458 mark (blue triangle), the positions of the COB interpretations (blue circles), the average COT
 459 range (calculated as the average start and average end of the COT interpretations, thick red line)
 460 and the range of COT interpretations (red whiskers).

461

462 **8 Discussion and conclusions**

463 From our analysis, the areas of greatest interpretation diversity (which we equate with the areas
 464 of greatest uncertainty in interpretation) are located in the middle of the seismic section, where
 465 the continent-ocean boundary or transition takes place. Here the interpretation focus is on the
 466 placement of the Moho and Top Basement and their relationship to each other. This is
 467 emphasised by the range across all groups in thickness interpretations of the crust through this
 468 central part of the seismic section. This zone of greatest uncertainty lies within the average COT
 469 zone of the interpretations and the range of COBs identified. This uncertainty is also emphasised
 470 by the other interpreted elements that lie within this zone including exhumed mantle and
 471 serpentinised crust. Here we discuss what this means for the different model concepts and a
 472 Wisdom of Crowds type approach to interpretation of Continent-Ocean margins.

473 The features that we requested the groups to interpret (Top Basement, Moho, Faults) are
 474 relatively consistent in their placement irrespective of the underlying conceptual abrupt COB or
 475 diffuse COT model evoked in the interpretation. A similar range of crustal thicknesses and the
 476 average COB boundary falling in the centre of the average COT transition zone interpreted
 477 implies a unity in observation and interpretation of key elements. Two interpretations stand out
 478 from the others; the first, in which interpretation of the Moho is deeper beneath the continent
 479 than in the other interpretations; and the second, in which the crust does not have a significant

480 extent of thinned section and the change from apparent continental crust to oceanic crust is
481 relatively abrupt. However, these two groups did interpret the COB within the range of other
482 interpretations. In summary, differences in interpretations appear to be the result of other factors
483 and are not related to the abrupt COB or diffuse COT margin model implied.

484 Although the interpretations of the two model concepts, COB and COT, differ in how they deal
485 with the uncertainty in interpreting the margin area, what is striking about the comparative
486 analysis of multiple interpretations of this single dataset are the similarities. If we consider the
487 two modal interpretations in Figure 6, the similarities between them are most apparent, with little
488 divergence in the interpretation of the Moho and Top Basement. Yet, the placement of the COB
489 and the demarcation of the COT zone are quite distinct. The COB interpretations span a range
490 from 75 km to just over 140 km along the seismic section, and the average COT zone ranges
491 from 80 km to just under 130 km. If we consider the COT zone interpretations in more detail
492 (Figure 3c), the 11 interpretations appear to fall into three sets: (a) those that have the COT zone
493 starting at a point (40-50 km along the section), where the continental crust can be considered as
494 definitely thinned (average thickness of 10-15 km). (b) Those that interpret the start of the COT
495 zone where the crust is significantly thinned to 2-3 km thick, between 75 - 85 km. And (c) those
496 that start the transition between 108-110 km in the middle of the significantly thinned section of
497 crust. Of these transition zone starting points, only the second group (i.e. starting between 75 and
498 85 km) coincide with three of the interpreted continent-ocean boundary points (Figure 3a). This
499 area is located at the approximate end of the deepening of the basement and encompass the
500 greatest number of interpretations (three COB and seven COT interpretations). Krishna et al.
501 (2009) also identified the COB in this area, based on gravity data (Figure 6a).

502 The extent or end point of the interpreted COT zones also differ, but are mostly concentrated
503 between 110 and 145 km (nine COT and the remaining two COB interpretations) (Figure 3b).
504 This zone (110-145 km) also include three of the published abrupt COB interpretations (i.e.
505 Powell et al., 1988, Rao et al., 1997, Sinha et al., 2010) as well as the end point of the diffuse
506 COT interpretation by Nemčok et al. (2013). Despite the broad coincidence in starting and
507 ending positions of abrupt COB and diffuse COT interpretations, the variability is too high to tie
508 these interpretations to single identifiable geological features in the Moho or the Top Basement.
509 This interpretational variability is also evident in published interpretations of COB and COT for
510 the East India passive margin (Table 2). These published interpretations use a range of data
511 (gravity, magnetic, refraction and reflection seismic data) to support the interpretation of COB
512 and COT locations and are thus not due to the methods used to identify the different components
513 of the passive margin. What becomes apparent is that not only are we uncertain about the
514 underpinning processes of continent-ocean margin rifting and development, but in how we
515 define COB and COT zones and their location.

516 As purported by Eagles et al. (2015), the terms and the ‘competing’ conceptual models are
517 perhaps not useful given the uncertainty in what is happening in these zones to the crust and
518 therefore in how we define and interpret these binary model concepts. From our analysis of
519 interpretations of a single 2D seismic section through the East Indian Margin, we can infer that
520 abrupt COB and diffuse COT models are not single deterministic model concepts, but that a
521 range of possible models exists within them. In our opinion, the terms are useful in describing
522 end-member concepts, but not in applying them in a binary nature. To understand tectonics

523 requires consideration of the uncertainty or range of possible interpretations of images and data
524 types, and the reduction of the debate to binary choices is unhelpful.

525 The paper is framed around the potential of using a combined Wisdom of Crowds and expert
526 elicitation approach to determine an optimal interpretation, or interpretations for the two (COB
527 and COT) model concepts. The conventional Wisdom of Crowds approach (Surowiecky, 2005)
528 was not perfectly applicable here because of the nature of the research question; the data that can
529 be interpreted using different model concepts and therefore there is not a single deterministic
530 solution, or answer, to the question posed. We also employed groups of experts to complete the
531 interpretations rather than individuals, so in fact the experiment results feature a double crowd-
532 sourcing: from individuals to their groups, and from groups to the abrupt COB and diffuse COT
533 modal interpretations. However, we believe that the range in interpretations is representative of
534 the community as supported by comparison of our data with existing published interpretations
535 through the margin (Figure 7). Eight of the ten published interpretations are located within the
536 interpretation range resulting from our experiment, and, perhaps anecdotally, the published COB
537 interpretation by Veevers et al (line 6 in Figure 7) lies almost at the exact position of the average
538 location of the COB groups (blue star in Figure 7). The average COT zone gives a good
539 representation of the likely range in continent-ocean crust change, and the average COB
540 interpretation falling in the middle of this range supports that the resulting average models are, at
541 the very least, geologically plausible. However, in our opinion our results do not imply a greater
542 probability of actually being in the middle of this range, or that the COB/COT locations follow a
543 symmetrical bell-shaped probability distribution. As is the case with many expert elicitation
544 exercises of this sort (see for example Polson and Curtis, 2010), the value of the exercise is more
545 in understanding expert interpretation processes the and range of opinion and possible
546 interpretations, rather than producing any aggregated solution.

547 In summary, the interpretations highlight to us the uncertainties in using seismic image data to
548 determine processes operating at continent-ocean margins, that multiple interpretations can be
549 used to determine the extent of the possible continent-ocean crust change, and that the current
550 ‘competing’ model concepts of an abrupt COB or diffuse COT are helpful in thinking about
551 processes of continental rifting but that constraining interpretation of continental margins into
552 binary choices is not useful. Our experiment highlights the range of possible interpretations
553 within each concept and the range of interpretations and potential continental rifting processes.

554 Acknowledgments

555 The authors would like to thank the full SEISMIX organisation team and participants for
556 facilitating and taking part in the experiment. Ion is thanked for use of the seismic profile in the
557 experiments. Dr Eagles and Dr Pérez-Díaz for kindly sharing the interpretations of the E-India
558 margin. JA is funded by grant IJC2018-036074-I, funded by MCIN/AEI
559 /10.13039/501100011033.
560

561 Open Research

- 562 The IndiaSPAN-1000 2D regional seismic line used in this experiment is not available, but
 563 images of the line (with different display characteristics) have been published in the following
 564 articles:
- 565 Haupert, I., Manatschal, G., Decarlis, A. and Unternehr, P., 2016. Upper-plate magma-poor
 566 rifted margins: Stratigraphic architecture and structural evolution. *Marine and Petroleum
 567 Geology*, 69, pp. 241-261. url:
 568 <https://www.sciencedirect.com/science/article/abs/pii/S0264817215301215> (last accessed:
 569 03/10/2022).
- 570 Mangipudi, V.R., Goli, A., Desa, M., Tammisetty, R. and Dewangan, P., 2014. Synthesis of deep
 571 multichannel seismic and high resolution sparker data: Implications for the geological
 572 environment of the Krishna–Godavari offshore, Eastern Continental Margin of India. *Marine and
 573 petroleum geology*, 58, pp. 339-355.
 574 url: <https://www.sciencedirect.com/science/article/abs/pii/S0264817214002621> (last accessed:
 575 03/10/2022).
- 576 Nemčok, M., Sinha, S.T., Stuart, C.J., Welker, C., Choudhuri, M., Sharma, S.P., Misra, A.A.,
 577 Sinha, N., Venkatraman, S., 2013. East Indian margin evolution and crustal architecture:
 578 integration of deep reflection seismic interpretation and gravity modelling. *Geol. Soc. Lond.,
 579 Spec. Publ.* 369, 477–496. url: <https://www.lyellcollection.org/doi/10.1144/sp369.6> (last
 580 accessed: 03/10/2022).
- 581 Pindell, J., Graham, R. and Horn, B., 2014. Rapid outer marginal collapse at the rift to drift
 582 transition of passive margin evolution, with a Gulf of Mexico case study. *Basin Research*, 26(6),
 583 pp.701-725. url: <https://onlinelibrary.wiley.com/doi/10.1111/bre.12059> (last accessed:
 584 03/10/2022).
- 585

586 References

- 587 Alcalde, J., Bond, C. E., Johnson, G., Butler, R. W., Cooper, M. A., & Ellis, J. F., 2017a. The
 588 importance of structural model availability on seismic interpretation. *Journal of
 589 Structural Geology*, 97, 161-171.
- 590 Alcalde, J., Bond, C.E., Johnson, G., Ellis, J.F. and Butler, R.W., 2017b. Impact of seismic
 591 image quality on fault interpretation uncertainty. *GSA Today*, v. 27, no. 2, pp. 4-10.
- 592 Alcalde, J., Bond, C.E. and Randle, C.H., 2017c. Framing bias: The effect of figure presentation
 593 on seismic interpretation. *Interpretation*, 5(4), pp.T591-T605.
- 594 Alcalde, J., Bond, C.E., Johnson, G., Kloppenborg, A., Ferrer, O., Bell, R. and Ayarza, P., 2019.
 595 Fault interpretation in seismic reflection data: an experiment analysing the impact of
 596 conceptual model anchoring and vertical exaggeration. *Solid Earth*, 10, 1561-1662.

- 597 Alcalde, J., and Bond, C.E., 2022. Subjective uncertainty and biases: the impact on seismic data
598 interpretation. In: *Bell, R., Iacopini, D., and Vardy, M. Interpreting Subsurface Seismic*
599 *Data* (pp. 103-123). Elsevier 308 pages.
- 600 Bastia, R., Radhakrishna, M., Srinivas, T., Nayak, S., Nathaniel, D.M., and Biswal, T.K., 2010,
601 Structural and tectonic interpretation of geophysical data along the eastern continental
602 margin of India with special reference to the deep water petrolierous basins, *J. Asian*
603 *Earth Sci.*, 39, 608—619.
- 604 Berndt, C., 2005. Focused fluid flow in passive continental margins. *Philosophical Transactions*
605 *of the Royal Society A: Mathematical, Physical and Engineering Sciences*, 363(1837),
606 pp.2855-2871.
- 607 Blaich, O.A., Faleide, J.I. and Tsikalas, F., 2011. Crustal breakup and continent-ocean transition
608 at South Atlantic conjugate margins. *Journal of Geophysical Research: Solid*
609 *Earth*, 116(B1).
- 610 Bond, C.E., Gibbs, A.D., Shipton, Z.K. and Jones, S., 2007. What do you think this is?
611 “Conceptual uncertainty” in geoscience interpretation. *GSA today*, 17(11), p.4.
- 612 Bond, C.E., 2015. Uncertainty in structural interpretation: Lessons to be learnt. *Journal of*
613 *Structural Geology*, 74, pp.185-200.
- 614 Bond, C. E., Johnson, G., & Ellis, J. F. (2015). Structural model creation: the impact of data type
615 and creative space on geological reasoning and interpretation. *Geological Society,*
616 *London, Special Publications*, 421(1), 83-97.
- 617 Bouysse, P., et al., 2009. Geological map of the world at 1:25 M. 3rd edition. CGMW (2 sheets,
618 2009).
- 619 Bradley, D.C., 2008. Passive margins through earth history. *Earth-Science Reviews*, 91(1-4),
620 pp.1-26.
- 621 Brune, S., Williams, S.E., Butterworth, N.P. and Müller, R.D., 2016. Abrupt plate accelerations
622 shape rifted continental margins. *Nature*, 536(7615), pp.201-204.
- 623 Budescu, D. V., & Chen, E. (2015). Identifying expertise to extract the wisdom of
624 crowds. *Management Science*, 61(2), 267-280.
- 625 Causer, A., Pérez-Díaz, L., Adam, J., & Eagles, G. (2020). Uncertainties in break-up markers
626 along the Iberia–Newfoundland margins illustrated by new seismic data. *Solid*
627 *Earth*, 11(2), 397-417.
- 628 Chian, D. and Louden, K.E., 1994. The continent-ocean crustal transition across the southwest
629 Greenland margin. *Journal of Geophysical Research: Solid Earth*, 99(B5), pp.9117-9135.
- 630 Eagles, G., Pérez-Díaz, L. and Scarselli, N., 2015. Getting over continent ocean boundaries.
631 *Earth-Science Reviews*, 151, pp.244-265.

- 632 Faleide, T. S., Braathen, A., Lecomte, I., Mulrooney, M. J., Midtkandal, I., Bugge, A. J., &
633 Planke, S. (2021). Impacts of seismic resolution on fault interpretation: Insights from
634 seismic modelling. *Tectonophysics*, 816, 229008.
- 635 Franke, D., Barckhausen, U., Baristeas, N., Engels, M., Ladage, S., Lutz, R., Montano, J.,
636 Pellejera, N., Ramos, E.G. and Schnabel, M., 2011. The continent-ocean transition at the
637 southeastern margin of the South China Sea. *Marine and Petroleum Geology*, 28(6),
638 pp.1187-1204.
- 639 Franke, D., 2013. Rifting, lithosphere breakup and volcanism: Comparison of magma-poor and
640 volcanic rifted margins. *Marine and Petroleum geology*, 43, pp.63-87.
- 641 Gibbons, A.D., Whittaker, J.M. and Müller, R.D., 2013. The breakup of East Gondwana:
642 Assimilating constraints from Cretaceous ocean basins around India into a best-fit
643 tectonic model. *Journal of geophysical research: solid earth*, 118(3), pp.808-822.
- 644 Haupert, I., Manatschal, G., Decarlis, A. and Unternehr, P., 2016. Upper-plate magma-poor
645 rifted margins: Stratigraphic architecture and structural evolution. *Marine and Petroleum
646 Geology*, 69, pp.241-261.
- 647 Hoffman, L.R. and Maier, N.R., 1961. Quality and acceptance of problem solutions by members
648 of homogeneous and heterogeneous groups. *The Journal of Abnormal and Social
649 Psychology*, 62(2), p.401.
- 650 Keen, C.E. and De Voogd, B., 1988. The continent-ocean boundary at the rifted margin off
651 eastern Canada: New results from deep seismic reflection studies. *Tectonics*, 7(1),
652 pp.107-124.
- 653 Kelley, H.H. and Thibaut, J.W., 1954. Experimental studies of group problem solving and
654 process. *Handbook of social psychology*, 2, pp.735-785.
- 655 Kittur, A. and Kraut, R.E., 2008, November. Harnessing the wisdom of crowds in wikipedia:
656 quality through coordination. In *Proceedings of the 2008 ACM conference on Computer
657 supported cooperative work* (pp. 37-46).
- 658 Krishna, K.S., Michael, L., Bhattacharyya, R. and Majumdar, T.J., 2009. Geoid and gravity
659 anomaly data of conjugate regions of Bay of Bengal and Enderby Basin: New constraints
660 on breakup and early spreading history between India and Antarctica. *Journal of
661 Geophysical Research: Solid Earth*, 114(B3).
- 662 Larrick, R. P., Mannes, A. E., & Soll, J. B. (2012). The social psychology of the wisdom of
663 crowds. In J. I. Krueger (Ed.), *Social judgment and decision making* (pp. 227–242).
664 Psychology Press.
- 665 Larson Jr, J.R., 2007. Deep diversity and strong synergy: Modeling the impact of variability in
666 members' problem-solving strategies on group problem-solving performance. *Small
667 Group Research*, 38(3), pp.413-436.

- 668 Lavier, L.L. and Manatschal, G., 2006. A mechanism to thin the continental lithosphere at
669 magma-poor margins. *Nature*, 440(7082), p.324.
- 670 Macrae, E. J., Bond, C. E., Shipton, Z. K., & Lunn, R. J. (2016). Increasing the quality of seismic
671 interpretation. *Interpretation*, 4(3), T395-T402.
- 672 Mangipudi, V.R., Goli, A., Desa, M., Tammisetty, R. and Dewangan, P., 2014. Synthesis of deep
673 multichannel seismic and high resolution sparker data: Implications for the geological
674 environment of the Krishna–Godavari offshore, Eastern Continental Margin of India.
675 *Marine and petroleum geology*, 58, pp.339-355.
- 676 Minshull, T.A., 2009. Geophysical characterisation of the ocean–continent transition at magma-
677 poor rifted margins. *Comptes Rendus Geoscience*, 341(5), pp.382-393.
- 678 Nemčok, M., Sinha, S.T., Stuart, C.J., Welker, C., Choudhuri, M., Sharma, S.P., Misra, A.A.,
679 Sinha, N., Venkatraman, S., 2013. East Indian margin evolution and crustal architecture:
680 integration of deep reflection seismic interpretation and gravity modelling. *Geol. Soc.
681 Lond., Spec. Publ.* 369, 477–496.
- 682 Pérez-Díaz, L., Alcalde, J., & Bond, C. E. (2020). Introduction: Handling uncertainty in the
683 geosciences: identification, mitigation and communication. *Solid Earth*, 11(3), 889-897.
- 684 Peron-Pinvidic, G., Manatschal, G. and Osmundsen, P.T., 2013. Structural comparison of
685 archetypal Atlantic rifted margins: A review of observations and concepts. *Marine and
686 Petroleum Geology*, 43, pp.21-47.
- 687 Pindell, J., Graham, R. and Horn, B., 2014. Rapid outer marginal collapse at the rift to drift
688 transition of passive margin evolution, with a Gulf of Mexico case study. *Basin Research*,
689 26(6), pp.701-725.
- 690 Polson, D. and Curtis, A., 2010. Dynamics of uncertainty in geological interpretation. *Journal of
691 the Geological Society*, 167(1), pp.5-10.
- 692 Powell, C.M., Roots, S.R., Veevers, J.J., 1988. Pre-breakup continental extension in east
693 Gondwanaland and the early opening of the eastern Indian Ocean. *Tectonophysics* 155,
694 261–283.
- 695 Rankey, E. C., & Mitchell, J. C. (2003). That's why it's called interpretation: Impact of horizon
696 uncertainty on seismic attribute analysis. *The Leading Edge*, 22(9), 820-828.
- 697 Rao, D.G., Krishna, K.S., Sar, D., 1997. Crustal evolution and sedimentation history of the Bay
698 of Bengal since the cretaceous. *J. Geophys. Res.* 102, 17747–17768.
699 <http://dx.doi.org/10.1029/96JB01339>.
- 700 Rao, G.S., Radhakrishna, M., 2014. Crustal structure and nature of emplacement of the 85° E
701 ridge in the Mahanadi offshore based on constrained potential field modeling:
702 implications for intraplate plume emplaced volcanism. *J. Asian Earth Sci.* 85, 80–96.

- 703 Schaaf, A., & Bond, C. E. (2019). Quantification of uncertainty in 3-D seismic interpretation:
704 implications for deterministic and stochastic geomodeling and machine learning. *Solid
705 earth*, 10(4), 1049-1061.
- 706 Schneider, C.A., Rasband, W.S., Eliceiri, K.W. 2012. NIH Image to ImageJ: 25 years of image
707 analysis. *Nature Methods* 9, 671-675, 2012.
- 708 Seton, M., Müller, R.D., Zahirovic, S., Gaina, C., Torsvik, T., Shephard, G., Talsma, A., Gurnis,
709 M., Turner, M., Maus, S. and Chandler, M., 2012. Global continental and ocean basin
710 reconstructions since 200 Ma. *Earth-Science Reviews*, 113(3-4), pp.212-270.
- 711 Sibuet, J. C., Srivastava, S., & Manatschal, G., 2007. Exhumed mantle-forming transitional crust
712 in the Newfoundland-Iberia rift and associated magnetic anomalies. *Journal of
713 Geophysical Research: Solid Earth*, 112(B6).
- 714 Sinha, S.T., Nemcok, M., Choudhuri, M., Misra, A.A., Sharma, S.P., Sinha, N., Venkatraman,
715 S., 2010. The Crustal Architecture and Continental Break up of East India Passive
716 Margin: An Integrated Study of Deep Reflection Seismic Interpretation and Gravity
717 Modeling. AAPG Annual Convention & Exhibition, New Orleans, USA, CD-ROM.
- 718 Straume, E.O., Gaina, C., Medvedev, S., Hochmuth, K., Gohl, K., Whittaker, J.M., Abdul Fattah,
719 R., Doornenbal, J.C. and Hopper, J.R., 2019. GlobSed: Updated total sediment thickness
720 in the world's oceans. *Geochemistry, Geophysics, Geosystems*, 20(4), pp.1756-1772.
- 721 Subrahmanyam, V., Subrahmanyam, A.S., Murty, G.P.S. and Murthy, K.S.R., 2008.
722 Morphology and tectonics of Mahanadi Basin, northeastern continental margin of India
723 from geophysical studies. *Marine Geology*, 253(1-2), pp.63-72.
- 724 Surowiecki, J., 2005. The wisdom of crowds. Anchor, 336 p.
- 725 Veevers, J.J., 2009. Palinspastic (pre-rift and-drift) fit of India and conjugate Antarctica and
726 geological connections across the suture. *Gondwana Res.* 16, 90–108.
- 727 Zhixin, W.E.N., Hong, X.U., Zhaoming, W.A.N.G., Zhengjun, H., Chengpeng, S.O.N.G., Xi,
728 C.H.E.N. and Yonghua, W.A.N.G., 2016. Classification and hydrocarbon distribution of
729 passive continental margin basins. *Petroleum Exploration and Development*, 43(5),
730 pp.740-750.

Figure 1.

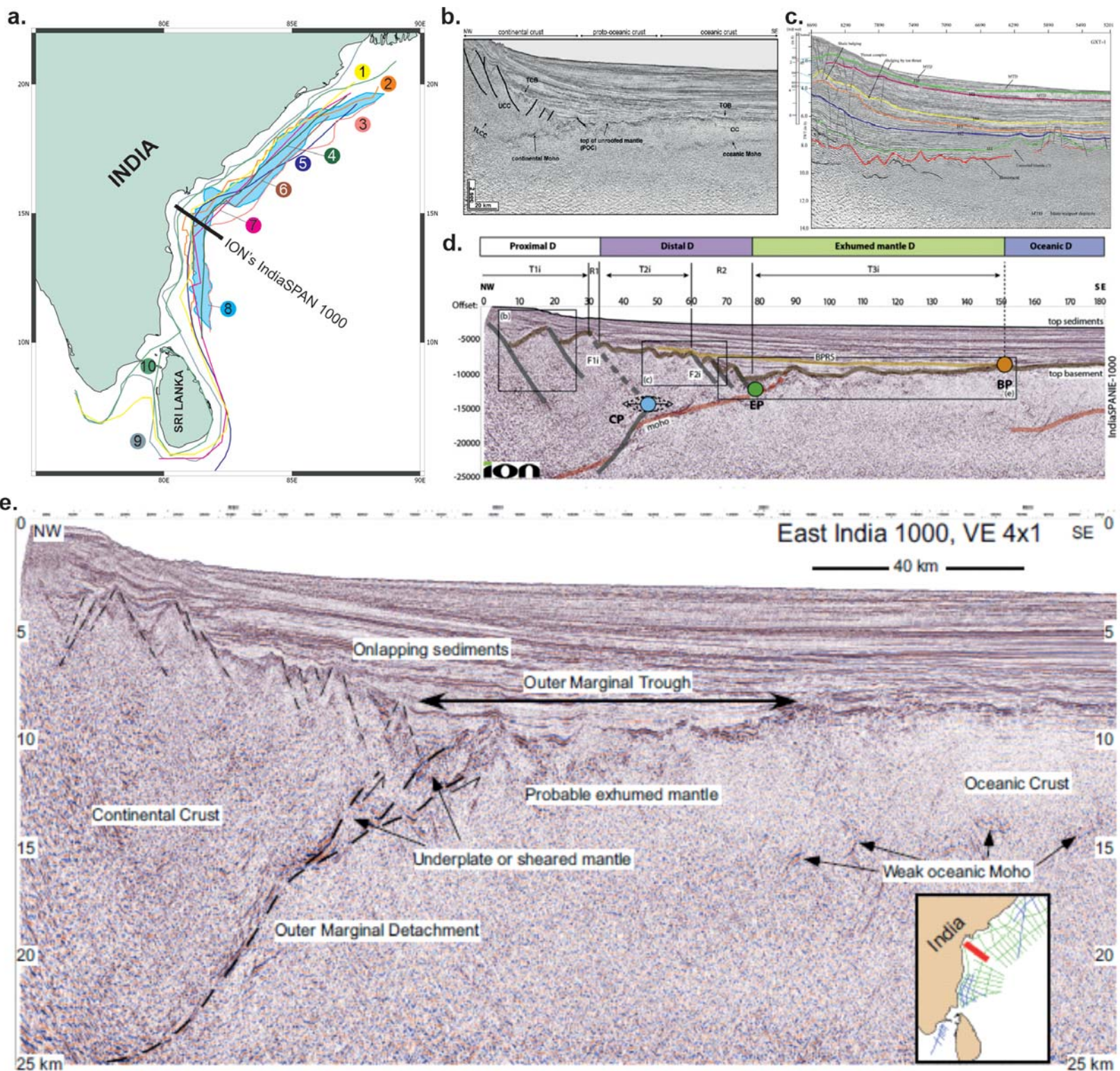


Figure 2.

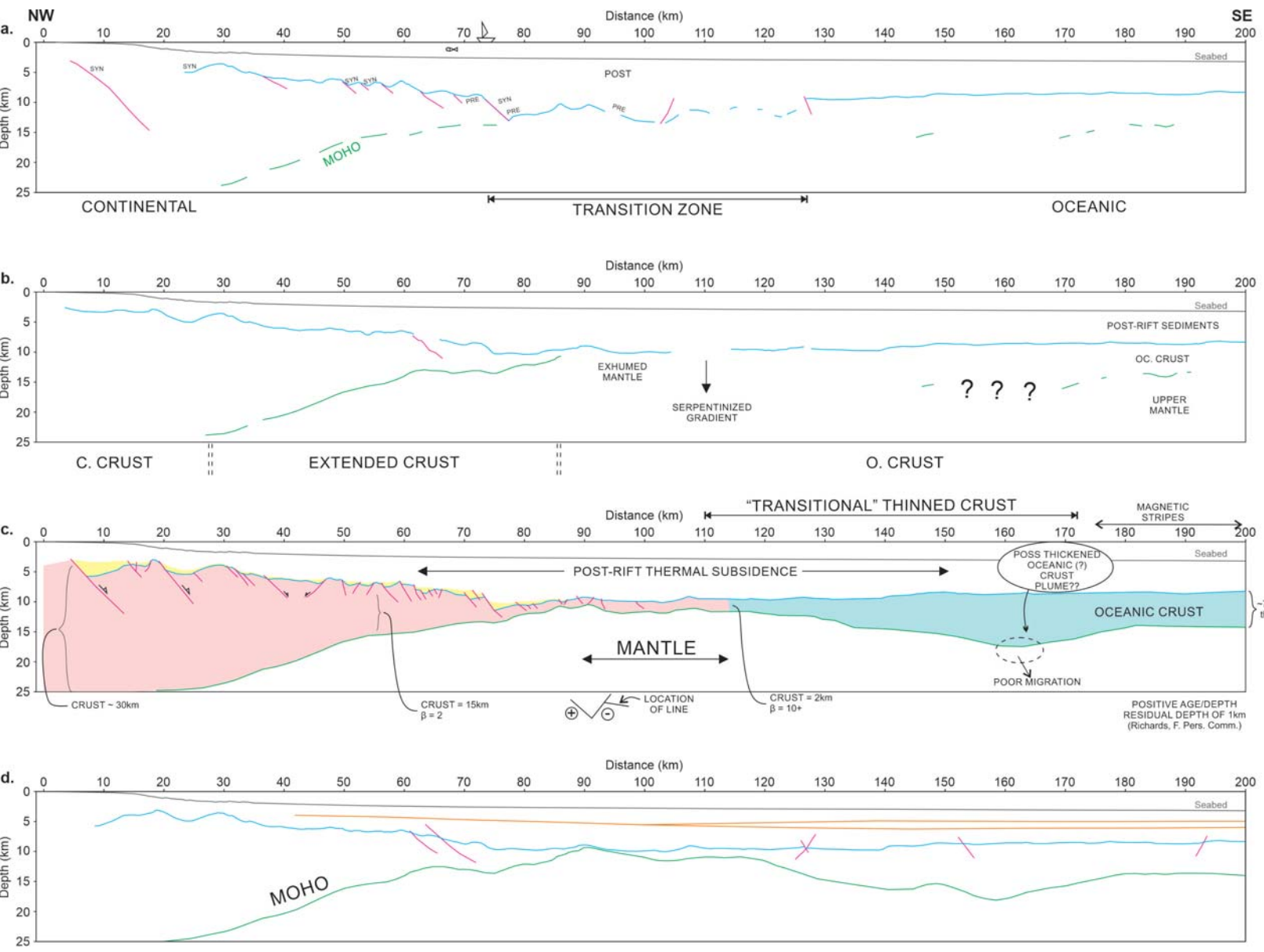


Figure 3.

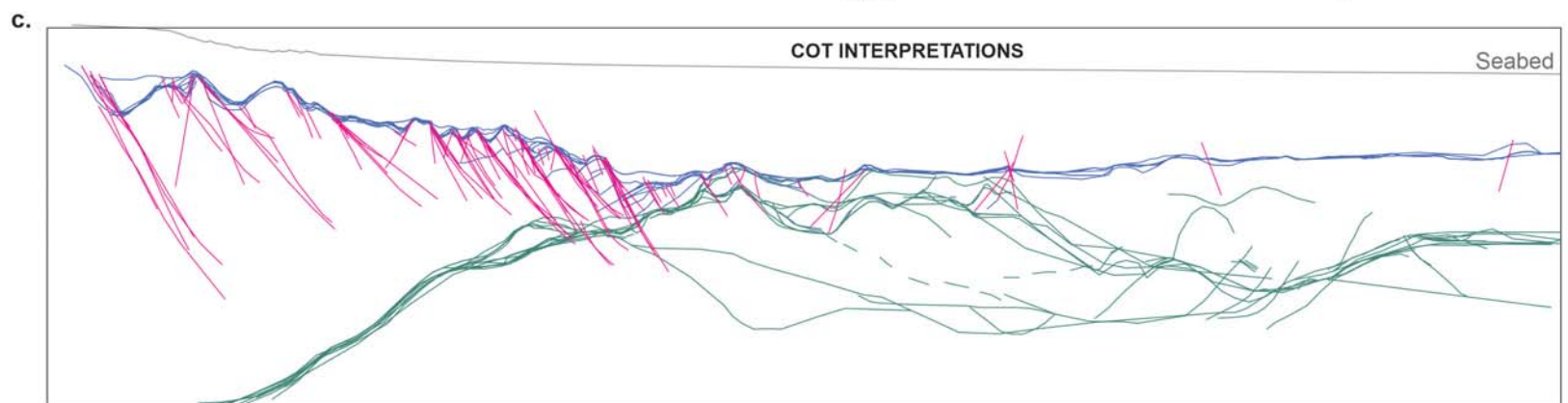
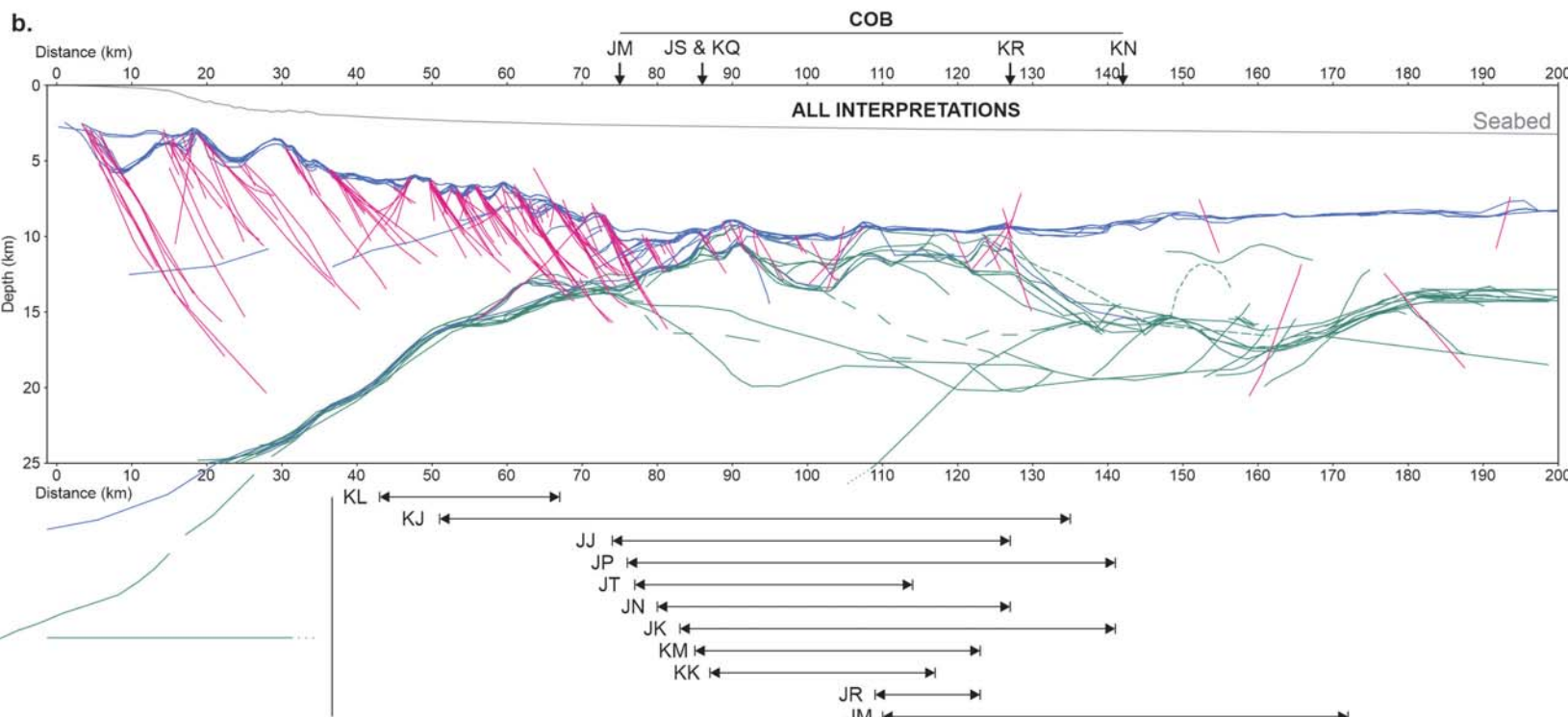
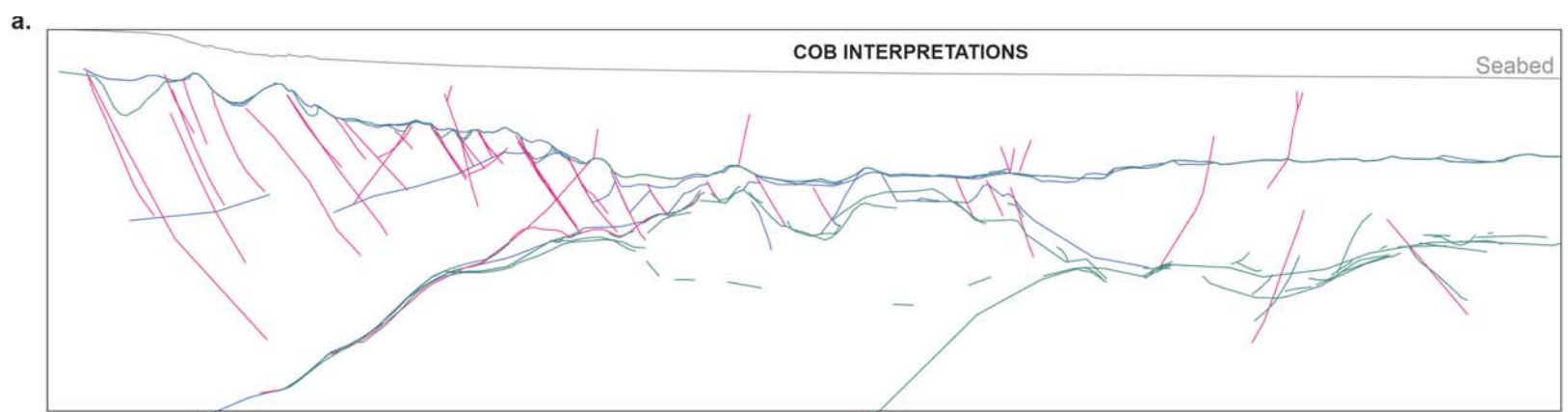


Figure 4.

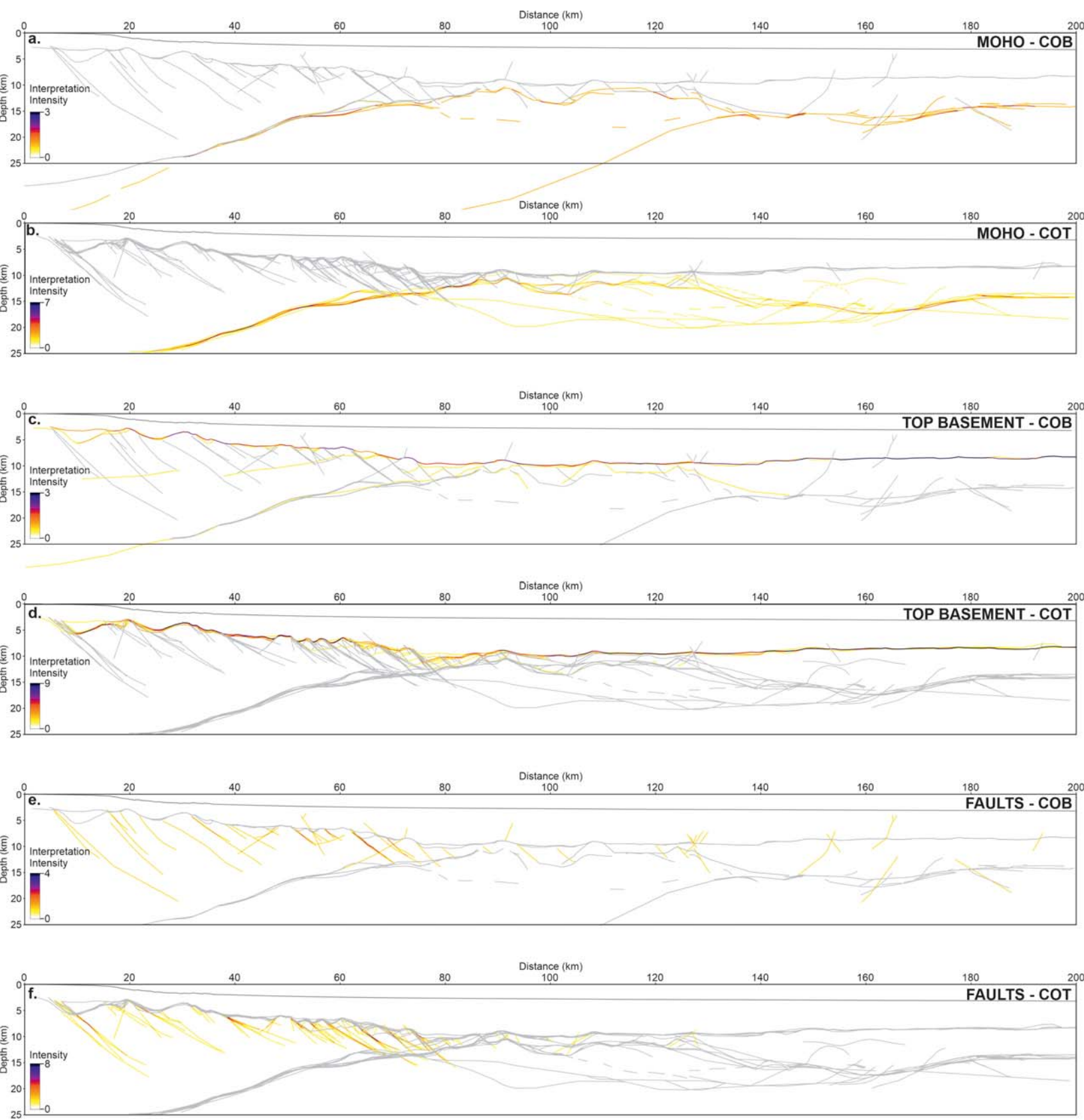


Figure 5.

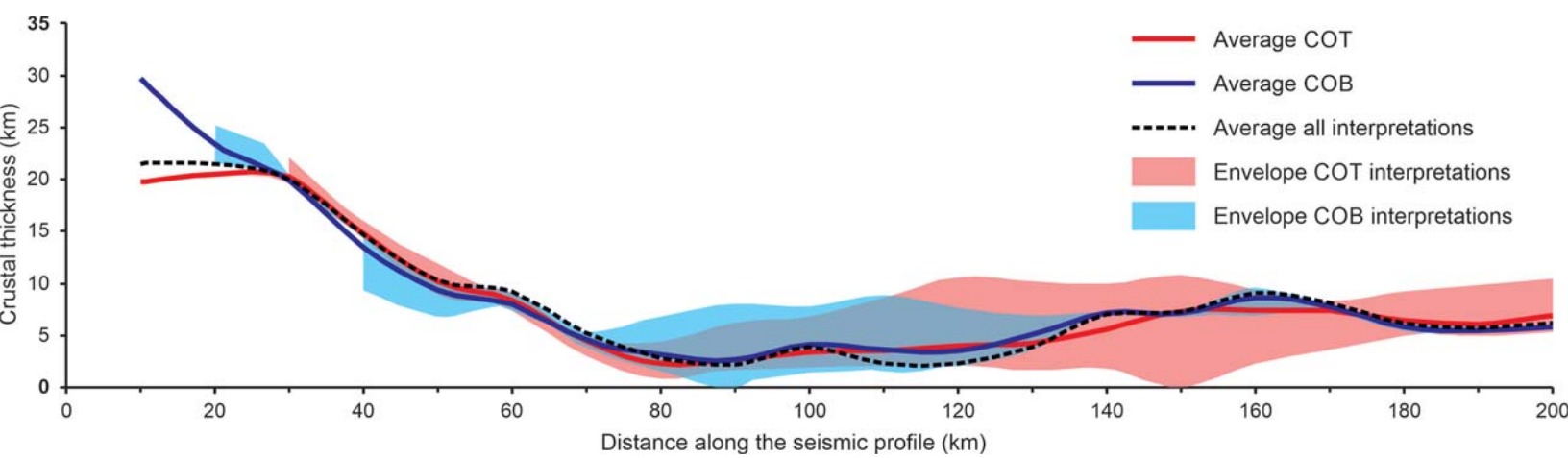


Figure 6.

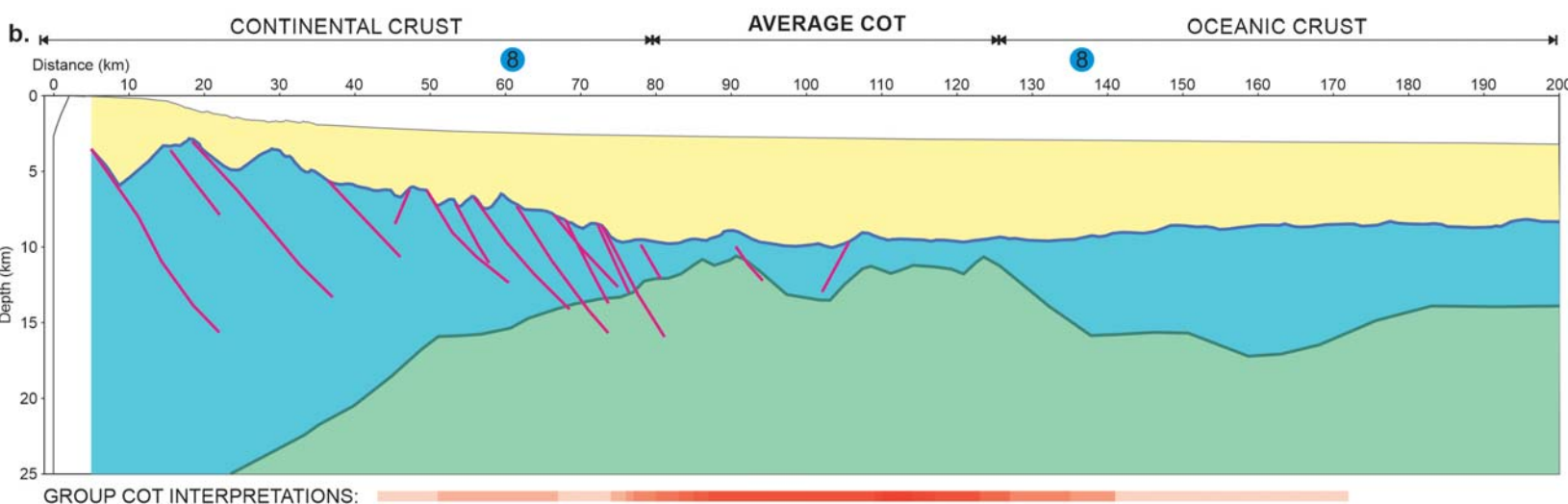
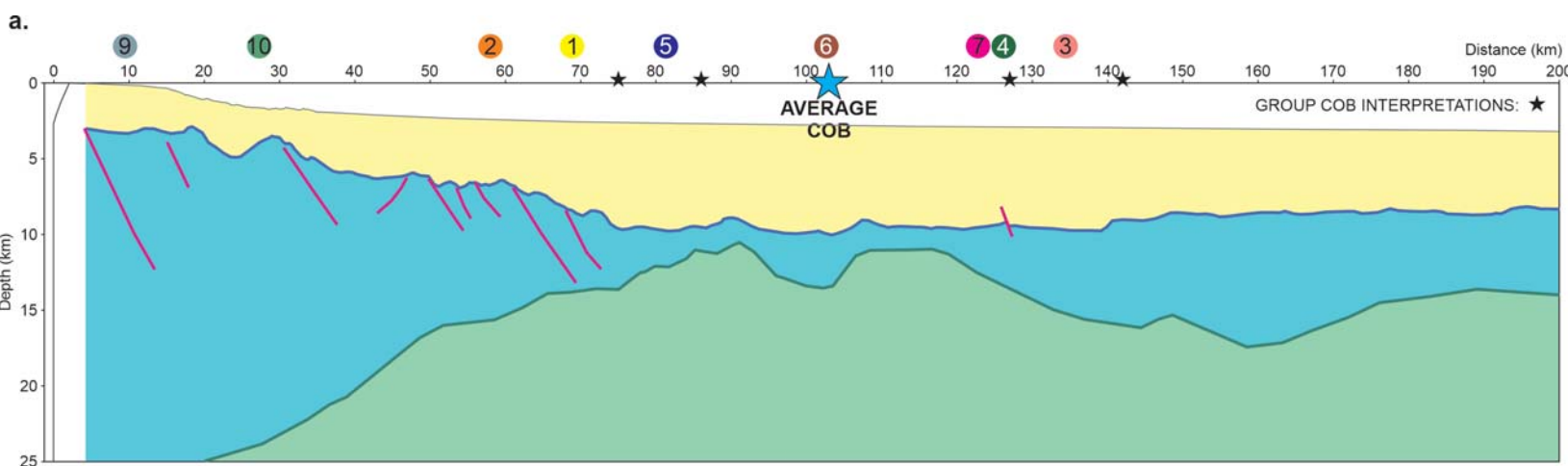


Figure 7.

